Desalination and Water Treatment
www.deswater.com

doi: 10.5004/dwt.2018.22234

110 (2018) 264–274
April

Effective removal of methyl violet dye using pomelo leaves as a new low-cost adsorbent

Linda B.L. Lim[a,*], Namal Priyantha[b,c], YieChen Lu[a], Nur Afiqah Hazirah Mohamad Zaidi[a]

[a]*Chemical Sciences, Faculty of Science, Universiti Brunei Darussalam, Jalan Tungku Link, Gadong, Negara Brunei Darussalam, Tel. +00 673 8748010; emails: linda.lim@ubd.edu.bn (L.B.L. Lim), yiechen_93@hotmail.com (Y.C. Lu), afhazirah@gmail.com (N.A.H. Mohamad Zaidi)*
[b]*Department of Chemistry, Faculty of Science, University of Peradeniya, Peradeniya, Sri Lanka*
[c]*Postgraduate Institute of Science, University of Peradeniya, Peradeniya, Sri Lanka, email: namal.priyantha@yahoo.com*

Received 8 November 2017; Accepted 23 March 2018

ABSTRACT

A new adsorbent, pomelo leaves (PL), was investigated as a possible low-cost adsorbent for the removal of toxic methyl violet (MV) dye. Adsorption isotherm data when fitted into five different models, namely the Langmuir, Freundlich, Temkin, Redlich–Peterson and Sips models, indicated the Sips model was the best fit with good maximum adsorption capacity (q_{max}) of 248.2 mg g^{-1}. Adsorption of MV by PL was an endothermic process and obeyed the pseudo-second order kinetics, showing a decrease in k_2 with increasing adsorbate concentration. PL's ability to adsorb MV was influenced by the presence of salts in solutions but is relatively resilient to changes in medium pH. An added attractive feature is its ability to be regenerated and reused, especially under both acid and base treatment, while maintaining good adsorption capacity even after five consecutive cycles. Thus, being readily available in abundance throughout the year, this study points to PL being a good, potential adsorbent in wastewater treatment given its high q_{max} when compared with many other adsorbents, pH resilience and that the spent adsorbent can be easily regenerated and reused.

Keywords: *Citrus grandis* (pomelo) leaf adsorbent; Methyl violet 2B dye; Adsorption characteristics; Isotherm; Kinetics; Regeneration

1. Introduction

Nowadays, due to the increase in industrialization, the amounts of pollutants being discharged as wastewater into the natural environment are on the rise as well. The untreated wastewater gives rise to serious environmental contamination. Amongst the various pollutants, one of the major contributors to water pollution is the availability of man-made dyes in the market place. Given that synthetic dyes cost less and offer a vast range of colours as compared with the natural dyes, they are gaining popularity and as a result have replaced many of the natural dyes. Untreated wastewater containing dyes not only is an eye-sore but also can cause imbalance in the aquatic ecosystem since these dyes, many of which are toxic, can interfere with photosynthesis and bio-accumulate in fish.

In recent years, many methods have been designed and developed to treat wastewater and these have been widely reported. Of these, a simple and yet effective method to remove various types of pollutants, for instance dyes and heavy metals, is adsorption. This technique is straight forward, low cost and has been proven to be successful in removing pollutants from wastewater. Reports have shown that low-cost adsorbents derived from industrial wastes [1,2], fruit wastes [3–6], leaves [7], agriculture wastes [8–11], peat [12–14], synthetic materials, aquatic plants [15], nanocomposites [16–19] and many others [20,21] have been successfully utilized.

* Corresponding author.

Methyl violet (MV) is a basic dye and is also known as methyl violet 2B or basic violet 1. It is commonly used in textile industry as well as in other industrial applications such as paper printing, inks, toners, leather, rubber or adhesives. However, despite its many uses, MV is a known carcinogenic dye with mutagenic properties and can cause skin irritation and eye damage, hinders the growth of microorganisms and photosynthesis of aquatic plants. Hence, there is a need for it to be removed from wastewater.

Citrus grandis, also known as *Citrus maxima*, is commonly known as pomelo, pummelo or shaddock. It belongs to the family of Rutaceae. The pomelo trees are now widely cultivated in Southeast Asia for its large fruits. There is no reported statistics on the annual production of pomelo fruit worldwide, however, the total production of grapefruit and pomelo covered 6.2% of total production of citrus in 1994 [22]. Also, in Malaysia, about 8,830 metric tons of pomelo fruits are produced annually with 1,895 hectare trees being grown for commercial use [23]. Normally, the flesh of the fruits is eaten while the peel is thrown away as waste. To date, reports have shown that pomelo peels have been successfully used for the removal of methylene blue [24], brilliant green [25], malachite green [26], congo red [27] and reactive blue 114 [28] dyes from aqueous solutions. Apart from dyes, pomelo peels have also been used to remove heavy metals such as copper [29], cadmium [30] and lead [31].

Amazingly, to the best of our knowledge, no report on the use of pomelo leaves (PL) has been published for the removal of synthetic dyes. Therefore, this is the first report on utilizing PL as a potential low-cost adsorbent. In this study, the focus is on the efficiency of PL as an adsorbent for the removal of toxic MV dye which includes the influence of contact time, medium pH, ionic strength, adsorption isotherm and kinetic mechanisms. PL will also be investigated for its regeneration and reusability potential as a low-cost adsorbent.

2. Materials and methods

2.1. Sample preparation and chemical reagents

The withered pomelo leaves (PL) collected from the ground of home garden were washed several times under tap water to remove any soil present, followed by washing with distilled water. PL were then dried in an oven at 65°C until a constant mass was obtained. Next, the dried samples were blended and sieved using laboratory stainless steel brass sieves to obtain the desired particle size of <355 μm which was used throughout this study. MV 2B dye of 80% purity (molecular formula of $C_{23}H_{26}N_3Cl$ and molecular weight of 379.93 g mol^{-1}) was purchased from Sigma-Aldrich Corporation, United Kingdom. All chemicals were used without further purification.

2.2. Adsorption experiments

In this study, effects of various parameters such as contact time (0–240 min), medium pH (4–10) and ionic strength (0–1 mol dm^{-3} of salt) were investigated on the extent of adsorption of MV on PL following the methods by Lim et al. [3]. In addition, the batch adsorption experiments for isotherm (0–1,000 mg L^{-1} of MV), kinetics and thermodynamic studies (temperature ranging from 298 to 343 K) were carried out. To investigate the ability to regenerate PL, studies were carried out for five consecutive cycles, adopting the method of Lim et al. [32]. For desorption, each of the five portions of spent PL was treated using 0.1 M HCl, 0.1 M NaOH, distilled water, washed quickly with distilled water and no treatment (as the control). All the experiments were carried out in duplicates using adsorbent:dye ratio of 1:500 (mass in gram:volume in mL), unless otherwise stated. Fig. 1 gives a pictorial presentation of the general adsorption experiment carried out using PL and MV dye.

3. Results and discussion

3.1. Characterization of PL

Surface morphology of PL investigated by SEM show a distinct difference before and after adsorption of MV dye (Fig. 2). Prior to adsorption of MV, the surface of PL appears rough and uneven with many irregularly shaped pores. Such uneven surface could provide favourable feature towards dye adsorption owing to increased surface area of the adsorbent. Once the PL was loaded with MV, there appeared to be a significant change in its surface morphology. Even though the surface still appears uneven, it is much smoother and majority of the pores, which initially were large and irregular, now appeared to have been covered.

Functional group characterization of PL based on Fourier-transform infrared (FTIR) spectroscopy (Fig. 3) reveals the presence of OH and amino groups at around 3,416 cm^{-1}, C–H, C=O and C=C at 2,926; 1,737 and 1,639 cm^{-1}, respectively. Band at 1,104 cm^{-1} could be due to C_{aliph}-N. Upon adsorption of MV dye, slight shift in OH from 3,416 to 3,421 cm^{-1} and C=O from 1,737 to 1,742 cm^{-1} were observed. Absorption bands at 1,587 and 1,170 cm^{-1} of dye-loaded PL are characteristics of C=C and C–H of aromatic rings of MV. Prominent changes occurred at 1,639 and 1,154 cm^{-1}, where upon MV adsorption, the bands were shifted to 1,659 and 1,174 cm^{-1}. Hence, C=O and C=C functional groups would probably be involved in the adsorption of MV dye. These functional groups present in the adsorbent would be attracted to MV through sharing of electrons between the adsorbent and adsorbate. Nevertheless, electrostatic attractions and ion exchange processes are unlikely to occur unlike in systems containing metal cations.

The point of zero charge (pH_{PZC}) of PL was determined to be at pH 5.02 (Fig. 4), suggesting that at this pH, the surface of PL has a zero charge. Protonation of the functional groups on the surface of PL will take place when the medium pH is below pH_{PZC}, thereby resulting in a predominantly positive surface. Under this condition, it is expected that there will be a decrease in adsorption towards MV as a result of electrostatic repulsion between the cationic MV dye and the positive surface. This is in fact what was observed when investigating the effect of medium pH on removal of MV by PL (see above). The reverse is true when the medium pH is greater than pH_{PZC}. Extent of adsorption of PL towards cationic MV dye increased at higher pH. However, unlike other reported adsorbents which are very much affected by medium pH, PL in general can be considered to be rather resilient to change in medium pH.

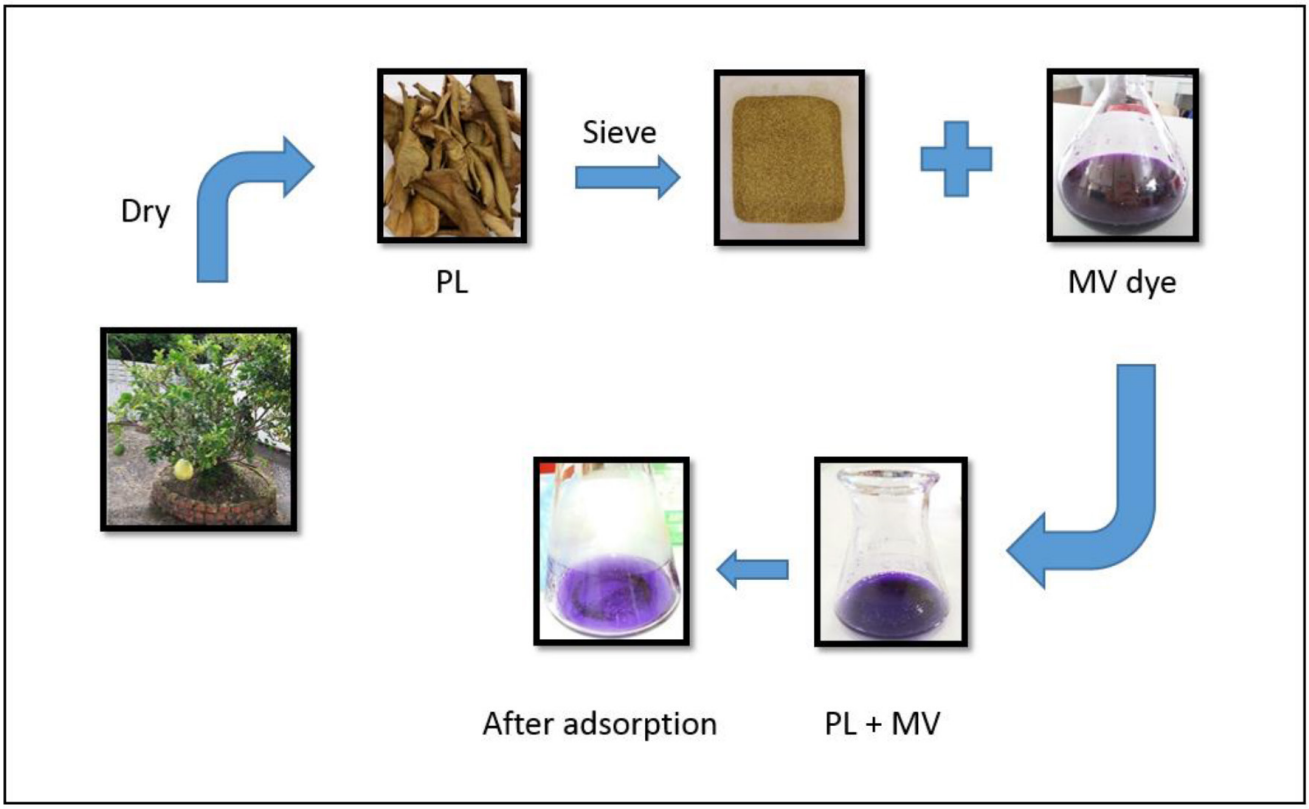

Fig. 1. Scheme showing the dried powder of PL and the dye solutions before and after adsorption process.

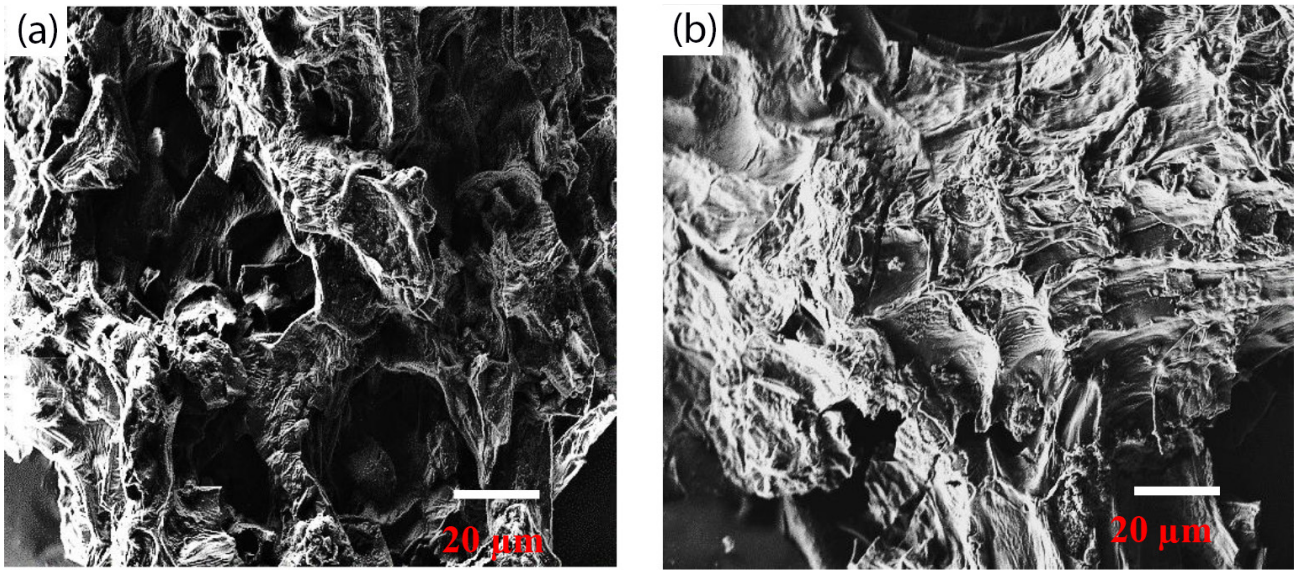

Fig. 2. Surface morphology, analyzed using SEM, of (a) PL and (b) MV-loaded PL at 800x magnification.

3.2. Effect of shaking time

Contact time is a crucial parameter in adsorption studies as it has great influence on the adsorption process. In this study, the time taken for the adsorbent–adsorbate system to reach equilibrium was investigated. As shown in Fig. 5, 150 min was sufficient for equilibrium to be reached. It can be observed in the figure that there is a rapid uptake of 100 mg L^{-1} MV dye within the first 30 min, which could be attributed to the initial availability of vacant sites on the surface of PL. Overtime, as the sites are being filled, the rate decreased and eventually reached a plateau, indicating that equilibrium has been reached. All subsequent experiments were carried out using 150 min as the contact time, unless

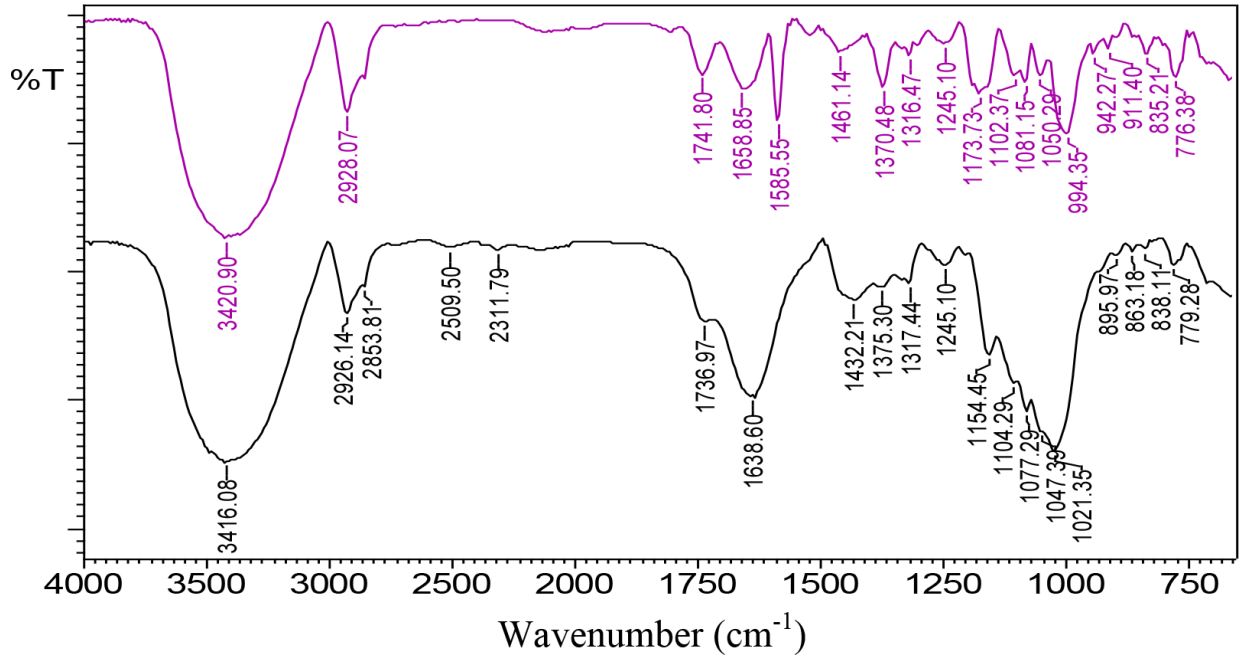

Fig. 3. FTIR spectra of PL (bottom – black) and MV-loaded PL (top – purple).

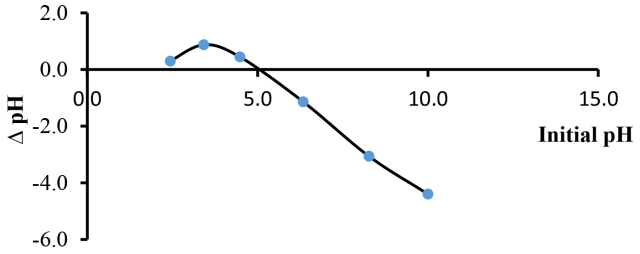

Fig. 4. Change in pH as a function of initial pH in order to determine the point of zero charge (pH_{PZC}) of PL (mass of adsorbent = 0.050 g; volume of solution = 25 mL).

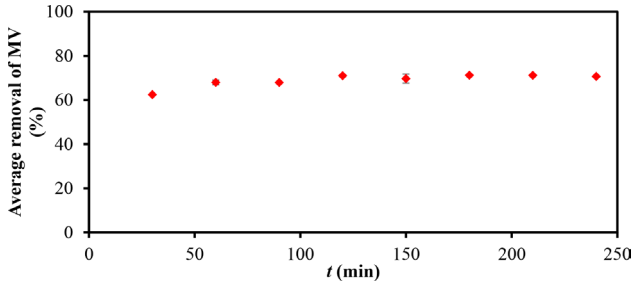

Fig. 5. Effect of contact time for the adsorption of MV onto PL (mass of adsorbent = 0.050 g; volume of MV solution = 25.0 mL, concentration of MV = 100 mg L^{-1}).

otherwise stated. PL shows its ability to reach equilibrium relatively fast when compared with other adsorbents such as water lettuce (180 min) [33], *Phragmites australis* (150–240 min) [34] and bagasse fly ash (240 min) [35].

3.3. Effect of pH on adsorption of MV onto PL

As reported by Kooh et al. [36], at higher pH, that is, greater than 11 and at acidic pH, that is, less than 2, the colour intensity of the MV dye is reduced. Hence, the chosen pH range in this study was limited to the range of pH 4–10. Two different dye concentrations (100 and 1,000 mg L^{-1}) were investigated. From Fig. 6, PL at untreated pH (4.14), was able to remove 37.8% of 100 mg L^{-1} MV dye. A decrease of 12% removal of MV was observed below the untreated pH, while above the untreated pH, there was a slight increase in removal of MV dye. Even though the removal of MV by PL was highest at pH 10 (42.9%), no adjustment of medium pH was deemed necessary in this study, and the untreated pH was used throughout since the difference in dye removal between the maximum removal and untreated pH was only 5%. This is due to the fact that MV is stable in the neutral form within a broad pH range from acidic to basic values, and it is protonated at very low pH. This explains the resistance of the adsorption power of PL to pH changes.

3.4. Effect of ionic strength

Four different salts (KCl, KNO_3, NaCl and $NaNO_3$), with concentrations ranging from 0 to 1.0 M, were used to examine the effect of ionic strength on the adsorption of MV dye by PL. From Fig. 7, it indicated that adsorption was least affected by KCl (~19% decrease at 1.0 mol dm^{-3}), and is followed by NaCl (~26%) and nitrate salts (~43%). Generally, reduction in the adsorption of cationic dyes with increasing salt concentration has been widely reported. Higher concentration of metal cations results in competition between these metal ions and the cationic dye molecules for the active sites on the adsorbent's surface.

3.5. Adsorption isotherm

In order to gain insight into the adsorption of MV on PL, batch adsorption isotherm experiments were carried out with dye concentration ranging from 10 to 1,000 mg L^{-1}

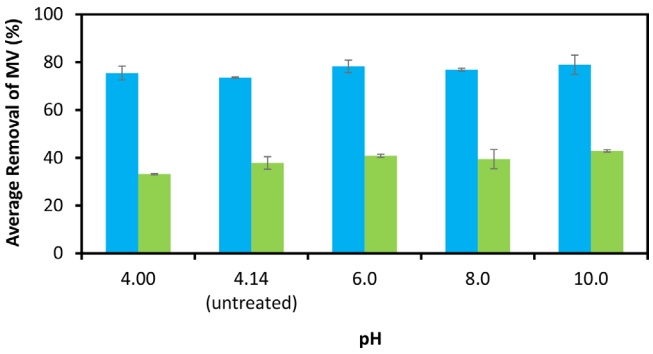

Fig. 6. Effect of pH on adsorption of MV onto PL in various medium pH (mass of adsorbent = 0.050 g; volume of MV = 25.0 mL; concentration of MV = 100 mg L^{-1} [■], 1,000 mg L^{-1} [■]).

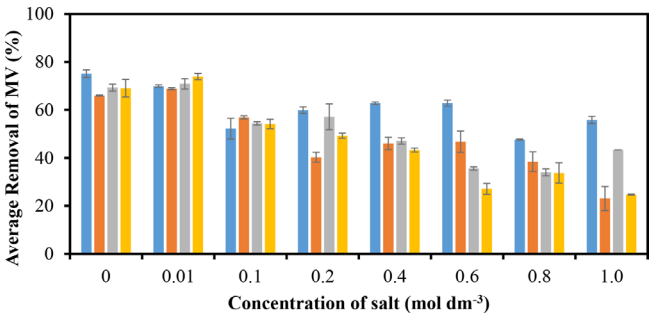

Fig. 7. Effect of ionic strength of KCl (■), KNO_3 (■), NaCl (■) and $NaNO_3$ (■) (mass of adsorbent = 0.050 g; volume of MV = 25.0 mL; concentration of MV = 100 mg L^{-1}).

to fit data for five different isotherm models, each having specific characteristics. For example, the Langmuir model [37] describes an adsorption process involving homogenous surface on which the adsorbates get adsorbed as a single monolayer. Thereafter, no further adsorption will take place. The Freundlich model [38], in contrast, applies to heterogeneous surface where adsorbates can be adsorbed as multilayers. The Temkin model [39] places its emphasis on the adsorbent–adsorbate interaction, ignoring the extremes of both high and low adsorbate concentrations and shows that the heat of adsorption decreases linearly with increase in surface coverage. In contrast to the above two parameter models, both the Redlich–Peterson (R–P) [40] and Sips [41] models are three parameter models and are combination of Langmuir and Freundlich models. The R–P model suggests that the adsorption process follows the Langmuir model at low adsorbate concentrations and it obeys the Freundlich model at higher concentrations. While, the reverse is true for the Sips model. Table 1 shows the equations of the models used for plotting the isotherm models based on the experimental data.

In order to find the best fit isotherm model for the adsorption of MV onto PL, three criteria namely coefficient of determinant (R^2), comparison of simulation plots with experiment data and error analyses that were performed using six error functions, whose equations are shown in Table 2 were used. Reports have shown that high R^2 values do not necessary point to the best fit model [42]. As shown in Table 3, the decreasing order of R^2 for the five isotherm models is Sips > Freundlich > Temkin > Langmuir > R–P. The R–P model has the lowest R^2 (0.5731) and its simulation plot in Fig. 8 clearly

Table 1
Linearized isotherm models used and their corresponding linear plots

Isotherm model	Linearized equation	Plot
Langmuir	$\frac{C_e}{q_e}=\frac{1}{K_L q_{\max}}+\frac{C_e}{q_{\max}}$	$\frac{C_e}{q_e}$ vs. C_e
	K_L is the Langmuir constant	
Freundlich	$\log q_e=\frac{1}{n}\log C_e+\log K_F$	log q_e vs. log C_e
	K_F is the Freundlich constant indicative of adsorption capacity; n is related to the adsorption intensity	
Temkin	$q_e=\left(\frac{RT}{b_T}\right)\ln K_T+\left(\frac{RT}{b_T}\right)\ln C_e$	q_e vs. lnC_e
	K_T is the Temkin constant; b_T is related to the heat of adsorption; R is the gas constant and T is the absolute temperature at 298 K	
Redlich–Peterson (R–P)	$\ln\left(\frac{K_R C_e}{q_e}-1\right)=n\ln C_e+\ln a_R$	$\ln\left(\frac{K_R C_e}{q_e}-1\right)$ vs. $\ln C_e$
	K_R and a_R are the R–P constants	
Sips	$\ln\left(\frac{q_e}{q_{\max}-q_e}\right)=\frac{1}{n}\ln C_e+\ln K_s$	$\ln\left(\frac{q_e}{q_{\max}-q_e}\right)$ vs. $\ln C_e$
	K_s is the Sips constant and n is the Sips exponent	

Table 2
List of various error functions used in this study

Type of errors	Equations
Average relative error (ARE)	$\frac{100}{n}\sum_{i=1}^{n}\left\lvert\frac{q_{e,\text{meas}}-q_{e,\text{calc}}}{q_{e,\text{meas}}}\right\rvert_i$
Sum square error (SSE)	$\sum_{i=1}^{n}\left(q_{e,\text{calc}}-q_{e,\text{meas}}\right)_i^2$
Hybrid fractional error function (HYBRID)	$\frac{100}{n-p}\sum_{i=1}^{n}\left[\frac{\left(q_{e,\text{meas}}-q_{e,\text{calc}}\right)^2}{q_{e,\text{meas}}}\right]_i$
Sum of absolute error (EABS)	$\sum_{i=1}^{n}\left\lvert q_{e,\text{meas}}-q_{e,\text{calc}}\right\rvert$
Marquardt's percent standard deviation (MPSD)	$100\sqrt{\frac{1}{n-p}\sum_{i=1}^{n}\left(\frac{q_{e,\text{meas}}-q_{e,\text{calc}}}{q_{e,\text{meas}}}\right)_i^2}$
Non-linear chi-square test (χ^2)	$\sum_{i=1}^{n}\frac{\left(q_{e,\text{meas}}-q_{e,\text{calc}}\right)^2}{q_{e,\text{meas}}}$

Table 3
Adsorption isotherm constants and error values of each isotherm model

Model	Values	ARE	SSE	HYBRID	EABS	MPSD	χ^2
Langmuir		12.74	0.05	0.74	0.60	21.75	0.29
q_{max} (mmol g^{-1})	0.77						
q_{max} (mg g^{-1})	303.17						
K_L (L mmol^{-1})	0.004						
R^2	0.8696						
Freundlich		18.95	0.24	3.00	1.13	30.53	0.52
K_F (mmol$^{1-1/n}$ L$^{1/n}$ g^{-1})	0.01						
K_F (mg$^{1-1/n}$ L$^{1/n}$ g^{-1})	2.06						
n	1.29						
R^2	0.9383						
Temkin		23.14	0.04	1.01	0.64	36.90	0.20
K_T (L mmol^{-1})	0.07						
b_T (J/mol)	16,605.06						
R^2	0.9438						
Redlich–Peterson		15.99	0.24	3.03	1.00	28.94	0.42
K_R (L g^{-1})	0.003						
α	0.66						
a_R (L mmol^{-1})	0.02						
R^2	0.5731						
Sips		8.41	0.02	0.39	0.40	14.66	0.17
q_{max} (mmol g^{-1})	0.63						
q_{max} (mg g^{-1})	248.19						
K_s (L mmol^{-1})	0.002						
$1/n$	1.29						
n	0.77						
R^2	0.9598						

shows that it is not the correct adsorption model in this study. Despite the high R^2 value for the Freundlich isotherm model, Fig. 8 clearly shows it deviated from the experiment data. This can be further confirmed by the high overall error values. The Freundlich model proposes a multilayer adsorption whereas the adsorption of MV by PL shows a plateau reaching at higher dye concentrations, indicating more of a monolayer adsorption process.

Of the three isotherm models left, the Temkin model has the highest error values which eliminate it from a suitable

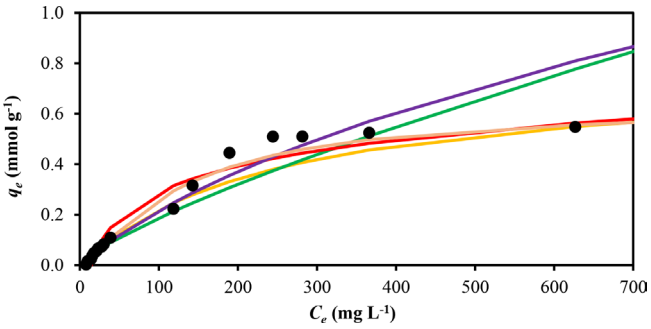

Fig. 8. Comparison of simulation plots of different types of isotherm models with experimental data such as Langmuir (▬), Freundlich (▬), Temkin (▬), R–P (▬), Sips (▬) and experimental data (●) (mass of adsorbent = 0.050 g; volume of MV = 25 mL; concentration of MV = 0 to 1,000 mg L^{-1}).

model. Between the Langmuir and the Sips models, the former has a lower R^2 with higher errors. Hence, in this study, adsorption of MV by PL is best described by the Sips model based on its high R^2 and low error values. As previously stated, the Sips model combines the Langmuir and Freundlich models, tending towards the Langmuir model at higher adsorbate concentrations.

Based on the Sips isotherm model, the maximum adsorption capacity (q_{max}) for the removal of MV by PL was found to be 248.2 mg g^{-1}. The q_{max} for monolayer adsorption based on the Langmuir model is 303.2 mg g^{-1}. Comparing this value with leaves of other reported plant materials, as shown in Table 4, it is clear that PL shows a much higher adsorption capacity towards MV. Its q_{max} based on monolayer adsorption is also better than the nanoparticle Pu-erh tea leaf, which also suggests that PL's adsorption capacity can be further enhanced since the current study utilizes bigger particle sizes of <350 μm. PL also exhibited better adsorption ability than other natural adsorbents such as almond shell, sunflower seed hull, etc. However, when compared with pomelo skin, the leaves have shown a lower q_{max} probably because of the difference in the texture of the two adsorbents. Pomelo skin is much thicker and spongier than its leaves. Nevertheless, PL can be considered to be a good adsorbent when compared with many other reported adsorbents.

Table 4
Comparison of the adsorption capacity (q_{max}) values of PL and some reported adsorbents used for the removal of MV dye

Adsorbent	q_{max} (mg g^{-1})	Reference
Citrus grandis (pomelo) leaf	248.2 (Sips)	This study
	303.2 (Langmuir)	
Citrus grandis (pomelo) skin	468.3	[43]
Pistia stratiotes L. (water lettuce)	267.6	[33]
Azolla pinnata	194.2	[36]
Nepenthes rafflesiana leaf	194.0	[44]
Mangrove leaf	78.0	[45]
Nanoparticle Pu-erh tea leaf	294.1	[46]
Acid-modified *Saccharum bengalense*	7.3	[47]
Posidonia oceanica L. leaf	119.1	[48]
Artocarpus odoratissimus (Tarap) leaf	139.7	[49]
Sunflower seed hull	93.0	[50]
Mansonia wood sawdust	16.0	[51]
Cempedak durian (*Artocarpus* sp.) peel	238.0	[52]
Artocarpus odoratissimus (Tarap) skin	137.3 (Sips)	[53]
Almond shell – untreated	29.4	[54]
– Magnetite-impregnated	33.0	
α-Fe_2O_3@porous hollow carbonaceous microspheres	539.8	[55]
Casuarina equisetifolia needle	165.0	[56]
Casuarina equisetifolia cone	63.0	[57]
Artocarpus odoratissimus (Tarap) stem axis	263.7	[58]
Artocarpus heterophyllus (jackfruit) seed	126.7	[59]
Duckweed	307.3 (Sips)	[60]
	332.5 (Langmuir)	
Nanocomposite	378.8	[61]

3.6. Thermodynamics of adsorption of MV onto PL

The thermodynamic parameters can be determined by using the van't Hoff equation, Eq. (3), by combining the Gibbs free energy, shown in Eq. (1), and the Gibbs free energy isotherm in Eq. (2).

$$\Delta G^\circ = \Delta H^\circ - T\Delta S^\circ \quad (1)$$

$$\Delta G^\circ = -RT\ln K_c, K_c = \frac{C_s}{C_e} \quad (2)$$

$$\ln K_c = \frac{\Delta S^\circ}{R} - \frac{\Delta H^\circ}{RT} \quad (3)$$

Based on the plot of ln K_c vs. 1/T from Eq. (3), the slope and intercept of the plot can be used to calculate the enthalpy (ΔH°), Gibbs free energy (ΔG°) and entropy (ΔS°) values. The plot is shown in Fig. 9.

Under the conditions employed, the adsorption of MV onto PL is endothermic in nature as the enthalpy (ΔH°) values are calculated to be positive. Although standard Gibbs free energy values (ΔG°) calculated based on thermodynamic arguments are positive, decrease in ΔG° with the increase in temperature from 298 to 343 K, small magnitudes of ΔG°, positive standard entropy change in adsorption (ΔS°), and differences between standard and ambient conditions employed in the study suggest that adsorption of MV onto PL be favourable depending on experimental conditions and spontaneous (Table 5). This is correspondently supported by the positive Freundlich constant (n = 1.29) which indicates that the adsorption process of MV onto PL is thermodynamically favourable, and by the sufficiently large q_{max} value determined in the study as compared with that of many other adsorbents. Positive entropy (ΔS°) value shows a possibility of significant changes in the internal structure of PL. It also indicates that during the adsorption process, there may be an increase in randomness between the interface of PL and MV. As the variation in Gibbs free energy is not much temperature dependent, and as extension of the proposed methodology for real applications would be performed under ambient conditions, investigation of adsorption characteristics of MV onto PL at warmer temperatures was not elaborated.

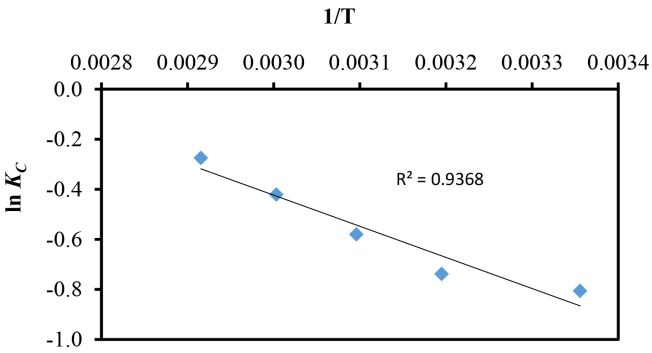

Fig. 9. Plot of van't Hoff for the adsorption of MV onto PL at 100 mg L^{-1} (♦) concentration of MV (mass of adsorbent = 0.050 g; volume of MV = 25.0 mL).

3.7. Adsorption kinetics of MV onto PL

In order to understand the adsorption kinetics of PL, the data obtained were modelled with the Lagergren pseudo-first order [62] and pseudo-second order [63] kinetics, whose linear equations are shown in Eqs. (5) and (6), respectively. Plots for both these two models (log ($q_e - q_t$) vs. t for pseudo-first order and t/q_t *vs.* t for pseudo–second order) are shown in Fig. 10.

Lagergren pseudo-first order:

$$\log(q_e - q_t) = \log(q_e) - \frac{k_1}{2.303}t \quad (5)$$

Pseudo-second order:

$$\frac{t}{q_t} = \frac{q}{k_2 q_e^2} + \frac{1}{q_e}t \quad (6)$$

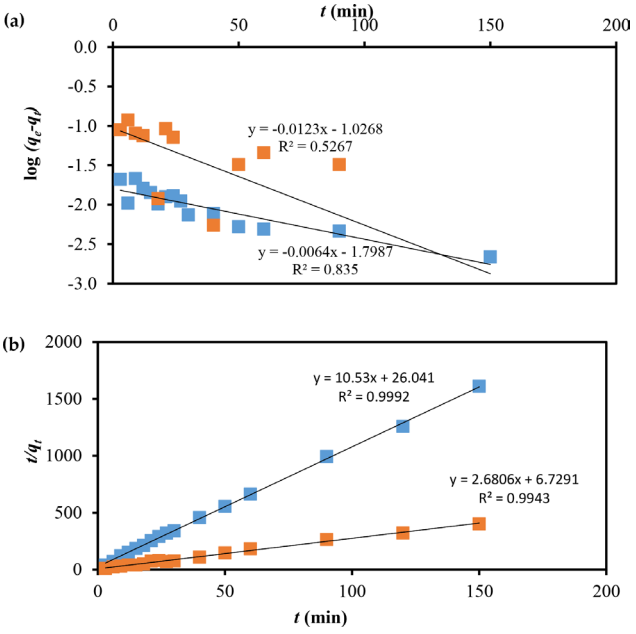

Fig. 10. Linear plots of (top) Lagergren first order and (bottom) pseudo-second order models for the adsorption of MV onto PL at 100 mg L^{-1} (■) and 500 mg L^{-1} (■) concentration of MV (mass of adsorbent = 0.050 g; volume of MV = 25.0 mL).

Table 5
Values of thermodynamic parameters for the adsorption of MV onto PL

Concentration	ΔH°	ΔS°	ΔG° (kJ mol^{-1})					R^2
(mg L^{-1})	(kJ mol^{-1})	(J mol^{-1} K^{-1})	298 K	313 K	323 K	333 K	343 K	
100	10.35	27.52	2.00	1.92	1.56	1.17	0.78	0.937

Table 6 clearly indicates that the pseudo-second order, with R^2 close to unity and smaller overall error values, is a better fit model. This is further confirmed by the compatible q_{calc} and q_{expt} values for the pseudo-second order kinetics whereas for the Lagergren pseudo-first order kinetics the q_{calc} and q_{expt} values showed a large discrepancy. Simulation plots of experimental data with both models, as shown in Fig. 11, also indicate that the pseudo-second order kinetics is the best fit model as compared with the Lagergren pseudo-first order model. Decrease in the values of k_2 with increase in the concentration of MV from 100 to 500 mg L^{-1} is in line with pseudo-second order kinetics, where according to Plazinski et al. [64] as concentration increases it is expected that equilibrium will require longer time to be reached. Further, Ho and McKay [65] have predicted the dependence of k_2 and adsorbate concentration.

3.8. Regeneration and reusability of PL

Generally, a spent adsorbent that can be regenerated and reused will give the adsorbent an added value in wastewater treatment application. In this study, spent PL were subjected to four different desorption methods and the adsorbent was then dried and reused. This is considered as one cycle. The study was repeated for five consecutive cycles and a control was also carried out for comparison purpose. It is observed from Fig. 12 that whether the PL were quickly rinsed with water or shaken in water did not make much difference in the adsorption of MV. Both gave relatively similar results. Spent PL which were not subjected to any treatment, as shown by the control, performed reasonably at cycle 2, but a drastic reduction in adsorption capability was observed at the end of the 5th cycle. However, both the acid and base treatments were able to maintain and even improve the adsorption capability of PL, with the latter being a better method. This could be due to base treatment results in the removal of surface wax and fats, thus exposing more functional groups on the surface which thereby enhances adsorption of dyes. Expansion of the pore structure is also possible with acid and base treatment enhancing the extent of removal of the adsorbate. The results obtained from acid treatment are similar with the result reported by Zhou et al. [66] whereby using HCl as the desorbing agent, the adsorption capacity of peach gum in removing MV only decreased by less than 10% after five cycles of desorption–adsorption [66]. Thus, the success in regenerating and reusing the spent PL is another favourable criterion for it to be used as a potential adsorbent.

Table 6
Kinetic parameters and error values for the adsorption of MV onto PL at 100 and 500 mg L^{-1} concentrations of MV

Concentration (mg L^{-1})	100	500
Pseudo-first order kinetics		
q_{calc} (mmol g^{-1})	0.016	0.094
q_{expt} (mmol g^{-1})	0.096	0.410
k_2 (min^{-1})	0.015	0.028
ARE	94.567	86.938
SSE	0.104	1.368
HYBRID	8.686	28.860
EABS	1.287	4.649
MPSD	101.127	93.096
χ^2	1.216	4.040
Pseudo-second order kinetics		
q_{calc} (mmol g^{-1})	0.095	0.373
q_{expt} (mmol g^{-1})	0.096	0.410
k_1 (g $mmol^{-1}$ min^{-1})	4.258	1.068
ARE	11.160	18.188
SSE	0.002	0.070
HYBRID	0.153	1.632
EABS	0.146	0.919
MPSD	13.834	23.315
χ^2	0.021	0.229

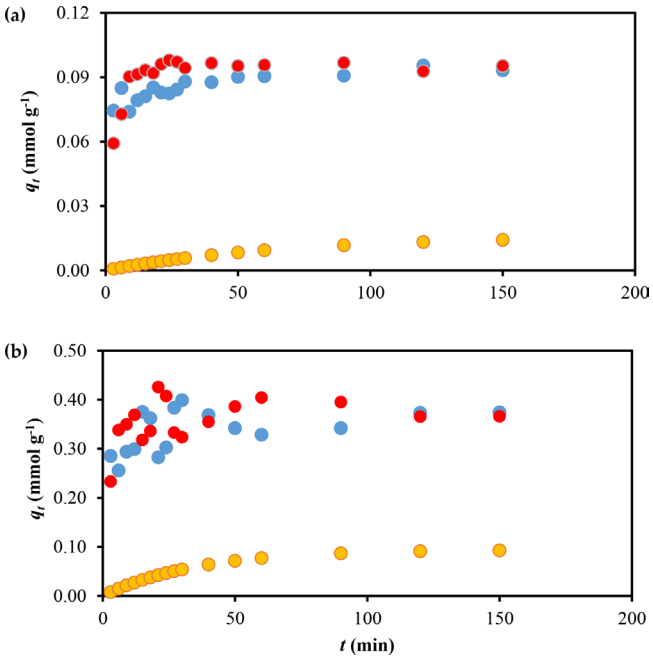

Fig. 11. Simulation plots of experimental data for kinetics (●), Lagergren first order (●) and pseudo-second order models (●) for the adsorption of MV onto PL at (a) 100 mg L^{-1} and (b) 500 mg L^{-1} concentration of MV (mass of adsorbent = 0.050 g; volume of MV = 25.0 mL).

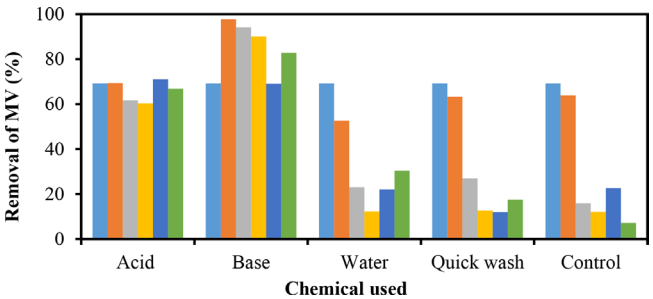

Fig. 12. Regeneration of PL for five consecutive cycles by treatment with different methods: cycle 0 (▪), cycle 1 (▪), cycle 2 (▪), cycle 3 (▪), cycle 4 (▪) and cycle 5 (▪) (mass of adsorbent = 0.050 g; concentration of MV = 250 mg L^{-1}).

4. Conclusion

Based on the results from this study, pomelo leaves, a newly reported adsorbent, indeed has great potential to be used in wastewater treatment application for the removal of methyl violet dye. Being readily available and in great abundance throughout the year, it is an attractive alternative low-cost adsorbent with high maximum adsorption capacity when compared with many reported natural adsorbents, and is relatively resilient to change in medium pH. Its ability to regenerate and reuse, especially under both acid and base conditions, while maintaining good adsorption ability for at least five consecutive cycles offers another attractive feature as a potential adsorbent.

Acknowledgements

The authors are grateful to the Government of Negara Brunei Darussalam, the Universiti Brunei Darussalam, and CAMES for their continuous support.

References

[1] A. Jain, V. Gupta, A. Bhatnagar, Utilization of industrial waste products as adsorbents for the removal of dyes, J. Hazard. Mater., 101 (2003) 31–42.
[2] A. Bhatnagar, A. Jain, A comparative adsorption study with different industrial wastes as adsorbents for the removal of cationic dyes from water, J. Colloid Interface Sci., 281 (2005) 49–55.
[3] L.B.L. Lim, N. Priyantha, T. Zehra, C.W. Then, C.M. Chan, Adsorption of crystal violet dye from aqueous solution onto chemically treated *Artocarpus odoratissimus* skin: equilibrium, thermodynamics, and kinetics studies, Desal. Wat. Treat., 57 (2016) 10246–10260.
[4] N. Priyantha, L.B.L. Lim, M.K. Dahri, Dragon fruit skin as a potent removal of manganese(II) ions, J. Appl. Sci. Environ. Sanit., 8 (2013) 179–188.
[5] L.A. Romero-Cano, H. García-Rosero, L.V. Gonzalez-Gutierrez, L.A. Baldenegro-Pérez, F. Carrasco-Marín, Functionalized adsorbents prepared from fruit peels: equilibrium, kinetic and thermodynamic studies for copper adsorption in aqueous solution, J. Clean. Prod., 162 (2017) 195–204.
[6] E.A. Khan, T.A. Khan, Adsorption of methyl red on activated carbon derived from custard apple (*Annona squamosa*) fruit shell: equilibrium isotherm and kinetic studies, J. Mol. Liq., 249 (2018) 1195–1211.
[7] L.B.L. Lim, N. Priyantha, H.I. Chieng, N.A.H.M. Zaidi, Adsorption characteristics of *Artocarpus odoratissimus* leaf toward removal of toxic Crystal violet dye: isotherm, thermodynamics and regeneration studies, J. Environ. Biotechnol. Res., 4 (2016) 32–40.
[8] D. Sud, G. Mahajan, M. Kaur, Agricultural waste material as potential adsorbent for sequestering heavy metal ions from aqueous solutions–a review, Bioresour. Technol., 99 (2008) 6017–6027.
[9] M.A.M. Salleh, D.K. Mahmoud, W.A.W.A. Karim, A. Idris, Cationic and anionic dye adsorption by agricultural solid wastes: a comprehensive review, Desalination, 280 (2011) 1–13.
[10] V.O. Njoku, M.A. Islam, M. Asif, B.H. Hameed, Utilization of sky fruit husk agricultural waste to produce high quality activated carbon for the herbicide bentazon adsorption, Chem. Eng. J., 251 (2014) 183–191.
[11] B. Hameed, F. Daud, Adsorption studies of basic dye on activated carbon derived from agricultural waste: *Hevea brasiliensis* seed coat, Chem. Eng. J., 139 (2008) 48–55.
[12] H.I. Chieng, L.B.L. Lim, N. Priyantha, D. Tennakoon, Sorption characteristics of peat of Brunei Darussalam III: equilibrium and kinetics studies on adsorption of crystal violet (CV), Int. J. Earth Sci. Eng., 6 (2013) 791–801.
[13] N. Priyantha, L.B.L. Lim, D.T.B. Tennakoon, H.I. Chieng, C. Bandara, Sorption characteristics of peat of Brunei Darussalam I: characterization of peat and adsorption equilibrium studies of methylene blue - peat interactions, Ceyl. J. Sci. (Physical Sciences), 17 (2013) 41–51.
[14] T. Zehra, L.B.L. Lim, N. Priyantha, Characterization of peat samples collected from Brunei Darussalam and their evaluation as potential adsorbents for Cu (II) removal from aqueous solution, Desal. Wat. Treat., 57 (2016) 20889–20903.
[15] B. Lu, Z. Xu, J. Li, X. Chai, Removal of water nutrients by different aquatic plant species: an alternative way to remediate polluted rural rivers, Ecol. Eng., 110 (2018) 18–26.
[16] G.R. Mahdavinia, H. Aghaie, H. Sheykhloie, M.T. Vardini, H. Etemadi, Synthesis of CarAlg/MMt nanocomposite hydrogels and adsorption of cationic crystal violet, Carbohydr. Polym., 98 (2013) 358–365.
[17] G.R. Mahdavinia, S. Iravani, S. Zoroufi, H. Hosseinzadeh, Magnetic and K^+-cross-linked kappa-carrageenan nanocomposite beads and adsorption of crystal violet, Iran. Polym. J., 23 (2014) 335–344.
[18] G.R. Mahdavinia, A. Massoudi, A. Baghban, B. Massoumi, Novel carrageenan-based hydrogel nanocomposites containing laponite RD and their application to remove cationic dye, Iran. Polym. J., 21 (2012) 609–619.
[19] G.R. Mahdavinia, F. Bazmizeynabad, B. Seyyedi, kappa-Carrageenan beads as new adsorbent to remove crystal violet dye from water: adsorption kinetics and isotherm, Desal. Wat. Treat., 53 (2015) 2529–2539.
[20] P. Sharma, H. Kaur, M. Sharma, V. Sahore, A review on applicability of naturally available adsorbents for the removal of hazardous dyes from aqueous waste, Environ. Monit. Assess., 183 (2011) 151–195.
[21] M. Ahmad, A.U. Rajapaksha, J.E. Lim, M. Zhang, N. Bolan, D. Mohan, M. Vithanage, S.S. Lee, Y.S. Ok, Biochar as a sorbent for contaminant management in soil and water: a review, Chemosphere, 99 (2014) 19–33.
[22] K.P. Paudyal, N. Haq, Variation of pomelo (*Citrus grandis* (L.) Osbeck) in Nepal and participatory selection of strains for further improvement, Agrofor. Syst., 72 (2008) 195–204.
[23] K.Y. Foo, B.H. Hameed, Microwave assisted preparation of activated carbon from pomelo skin for the removal of anionic and cationic dyes, Chem. Eng. J., 173 (2011) 385–390.
[24] B. Hameed, D. Mahmoud, A. Ahmad, Sorption of basic dye from aqueous solution by pomelo (*Citrus grandis*) peel in a batch system, Colloids Surf., A, 316 (2008) 78–84.
[25] M.K. Dahri, M.R.R. Kooh, L.B.L. Lim, Adsorption characteristics of pomelo skin toward toxic Brilliant Green dye, Scientia Bruneiana, 16 (2017) 49–56.
[26] O.S. Bello, M.A. Ahmad, B. Semire, Scavenging malachite green dye from aqueous solutions using pomelo (*Citrus grandis*) peels: kinetic, equilibrium and thermodynamic studies, Desal. Wat. Treat., 56 (2015) 521–535.
[27] M. Jayarajan, R. Arunachalam, G. Annadurai, Use of low cost nano-porous materials of pomelo fruit peel wastes in removal of textile dye, Res. J. Environ. Sci., 5 (2011) 434–443.
[28] M.E. Argun, D. Güclü, M. Karatas, Adsorption of Reactive Blue 114 dye by using a new adsorbent: pomelo peel, J. Ind. Eng. Chem., 20 (2014) 1079–1084.
[29] N. Begum, A. Noorliyana, M.F. Bari, N.A. Halif, N. Hidayah, K.R. Ahmed, Kinetic and thermodynamic studies on adsorption of copper ions onto pomelo peel (*Citrus grandis*), Adv. Mater. Res., 795 (2013) 674–678.
[30] W. Saikaew, P. Kaewsarn, W. Saikaew, Pomelo peel: agricultural waste for biosorption of cadmium ions from aqueous solutions, World Acad. Sci. Eng., Technol., 56 (2009) 287–291.
[31] J.-y. Liu, G.-h. Huang, J.-q. Deng, K. Liu, Y.-b. Xie, Adsorbent prepared from waste pomelo peel and its adsorption of Pb^{2+} in wastewater, J. Ecol. Rural Environ., 28 (2012) 187–191.
[32] L.B.L. Lim, N. Priyantha, N.H. Mohd Mansor, Utilizing *Artocarpus altilis* (breadfruit) skin for the removal of malachite green: isotherm, kinetics, regeneration, and column studies, Desal. Wat. Treat., 57 (2016) 16601–16610.

[33] L.B.L. Lim, N. Priyantha, C.M. Chan, D. Matassan, H.I. Chieng, M.R.R. Kooh, Investigation of the sorption characteristics of water lettuce (WL) as a potential low-cost biosorbent for the removal of methyl violet 2B, Desal. Wat. Treat., 57 (2016) 8319–8329.
[34] G.B. Kankılıç, A.Ü. Metin, İ. Tüzün, *Phragmites australis*: an alternative biosorbent for basic dye removal, Ecol. Eng., 86 (2016) 85–94.
[35] I.D. Mall, V.C. Srivastava, N.K. Agarwal, Removal of Orange-G and Methyl Violet dyes by adsorption onto bagasse fly ash—kinetic study and equilibrium isotherm analyses, Dyes Pigm., 69 (2006) 210–223.
[36] M.R.R. Kooh, L.B.L. Lim, M.K. Dahri, L.H. Lim, J.S. Bandara, *Azolla pinnata*: an efficient low cost material for removal of methyl violet 2B by using adsorption method, Waste Biomass Valorization, 6 (2015) 547–559.
[37] I. Langmuir, The adsorption of gases on plane surfaces of glass, mica and platinum, J. Am. Chem. Soc., 40 (1918) 1361–1403.
[38] H. Freundlich, Over the adsorption in the solution, J. Phys. Chem., 57 (1906) 385–470.
[39] M.J. Temkin, V. Pyzhev, Kinetics of ammonia synthesis on promoted iron catalysts, Acta Physiochim., 12 (1940) 217.
[40] O. Redlich, D.L. Peterson, A useful adsorption isotherm, J. Phys. Chem., 63 (1959) 1024–1024.
[41] R. Sips, Combined form of Langmuir and Freundlich equations, J. Chem. Phys., 16 (1948) 490–495.
[42] L.B.L. Lim, N. Priyantha, K.J. Mek, N.A.H.M. Zaidi, Potential use of *Momordica charantia* (bitter gourd) waste as a low-cost adsorbent to remove toxic crystal violet dye, Desal. Wat. Treat., 82 (2017) 121–130.
[43] M.K. Dahri, M.R.R. Kooh, L.B.L. Lim, Artificial neural network approach for modelling of methyl violet 2B dye adsorption using pomelo skin, J. Environ. Biotechnol. Res., 6 (2017) 238–247.
[44] M.R.R. Kooh, M.K. Dahri, L.B.L. Lim, Removal of methyl violet 2B dye from aqueous solution using *Nepenthes rafflesiana* pitcher and leaves, Appl. Water Sci., 7 (2017) 3859–3868.
[45] B. Bano, E. Zahir, Comparative study of raw and chemically treated mangrove leaf for remediation of 304 Methyl Violet 2B dye from aqueous solution: thermo-kinetics aspect, Water Sci. Technol., 73 (2016) 1301–1312.
[46] P. Li, Y.-J. Su, Y. Wang, B. Liu, L.-M. Sun, Bioadsorption of methyl violet from aqueous solution onto Pu-erh tea powder, J. Hazard. Mater., 179 (2010) 43–48.
[47] M.I. Din, K. Ijaz, K. Naseem, Biosorption potentials of acid modified *Saccharum bengalense* for removal of methyl violet from aqueous solutions, Chem. Ind. Chem. Eng. Q., 23 (2016) 54–54.
[48] S. Cengiz, L. Cavas, A promising evaluation method for dead leaves of *Posidonia oceanica* (L.) in the adsorption of methyl violet, Marine Biotechnol., 12 (2010) 728–736.
[49] L.B.L. Lim, N. Priyantha, N.A.H. Mohamad Zaidi, A superb modified new adsorbent, *Artocarpus odoratissimus* leaves, for removal of cationic methyl violet 2B dye, Environ. Earth Sci., 75 (2016) 1179.
[50] B.H. Hameed, Equilibrium and kinetic studies of methyl violet sorption by agricultural waste, J. Hazard. Mater., 154 (2008) 204–212.
[51] A.E. Ofomaja, Y.-S. Ho, Effect of temperatures and pH on methyl violet biosorption by Mansonia wood sawdust, Bioresour. Technol., 99 (2008) 5411–5417.
[52] M.K. Dahri, H.I. Chieng, L.B.L. Lim, N. Priyantha, C.C. Mei, Cempedak Durian (*Artocarpus* sp.) Peel as a biosorbent for the removal of toxic methyl violet 2b from aqueous solution, Korean Chem. Eng. Res., 53 (2015) 576–583.
[53] L.B.L. Lim, N. Priyantha, C.H. Ing, M.K. Dahri, D.T.B. Tennakoon, T. Zehra, M. Suklueng, *Artocarpus odoratissimus* skin as a potential low-cost biosorbent for the removal of methylene blue and methyl violet 2B, Desal. Wat. Treat., 53 (2015) 964–975.
[54] K. Saeed, M. Ishaq, S. Sultan, I. Ahmad, Removal of methyl violet 2-B from aqueous solutions using untreated and magnetite-impregnated almond shell as adsorbents, Desal. Wat. Treat., 57 (2016) 13484–13493.
[55] Z. Tong, P. Zheng, B. Bai, H. Wang, Y. Suo, Adsorption performance of methyl violet via α-Fe_2O_3@ porous hollow carbonaceous microspheres and its effective regeneration through a Fenton-like reaction, Catalysts, 6 (2016) 58.
[56] M.R.R. Kooh, M.K. Dahri, L.B.L. Lim, Removal of Methyl Violet 2B from aqueous solution using *Casuarina equisetifolia* needle, ISRN Environ. Chem., 2013 (2013) Article ID 619819.
[57] M.K. Dahri, M.R.R. Kooh, L.B.L. Lim, Water remediation using *Casuarina equisetifolia* cone as adsorbent for the removal of methyl violet 2B dye using batch experiment method, J. Environ. Biotechnol. Res., 6 (2017) 34–42.
[58] M.R.R. Kooh, M.K. Dahri, L.B.L. Lim, Removal of the methyl violet 2B dye from aqueous solution using sustainable adsorbent *Artocarpus odoratissimus* stem axis, Appl. Water Sci., 7 (2017) 3573–3581.
[59] M.K. Dahri, M.R.R. Kooh, L.B.L. Lim, Adsorption of toxic methyl violet 2B dye from aqueous solution using *Artocarpus heterophyllus* (Jackfruit) seed as an adsorbent, Am. Chem. Sci. J., 15 (2016) 1–12.
[60] L.B.L. Lim, N. Priyantha, C.M. Chan, D. Matassan, H.I. Chieng, M.R.R. Kooh, Adsorption behavior of methyl violet 2B using duckweed: equilibrium and kinetics studies, Arab. J. Sci. Eng., 39 (2014) 6757–6765.
[61] S. Ghorai, A. Sarkar, M. Raoufi, A.B. Panda, H. Schönherr, S. Pal, Enhanced removal of methylene blue and methyl violet dyes from aqueous solution using a nanocomposite of hydrolyzed polyacrylamide grafted xanthan gum and incorporated nanosilica, ACS Appl. Mater. Interface, 6 (2014) 4766–4777.
[62] S. Lagergren, About the theory of so-called adsorption of soluble substances, K. Sven. Vetensk.akad. Handl., 24 (1898) 1–39.
[63] Y.S. Ho, G. McKay, Sorption of dye from aqueous solution by peat, Chem. Eng. J., 70 (1998) 115–124.
[64] W. Plazinski, J. Dziuba, W. Rudzinski, Modeling of sorption kinetics: the pseudo-second order equation and the sorbate intraparticle diffusivity, Adsorption, 19 (2013) 1055–1064.
[65] Y.S. Ho, G. McKay, The kinetics of sorption of divalent metal ions onto sphagnum moss peat, Water Res., 34 (2000) 735–742.
[66] L. Zhou, J. Huang, B. He, F. Zhang, H. Li, Peach gum for efficient removal of methylene blue and methyl violet dyes from aqueous solution, Carbohydr. Polym., 101 (2014) 574–581.